NILU
OPPDRAGSRAPPORT NR: 1/81
REFERENCE: 222/79
DATE: JANUARY 1981

ON THE PREDICTION OF HAZARD AREA RESULTING FROM A GAS RELEASE

BY

KARL J. EIDSVIK

NORWEGIAN INSTITUTE FOR AIR RESEARCH
P.O. BOX 130, N-2001 LILLESTRØM
NORWAY

ISBN--82-7247-214-7

ON THE PREDICTION OF HAZARD AREA RESULTING FROM A GAS RELEASE

by

Karl J. Eidsvik
Norwegian Institute for Air Research
P.O. Box 130, N-2001 Lillestrøm

Abstract

A synthesis of hazard area prediction following the release of a hazardous gas cloud is developed. At a fixed risk level the predicted hazard area is estimated to depend much upon prediction errors for actual atmospheric transport and flow parameters.

1 Introduction

The basic theories of turbulent diffusion, developed by Taylor and Batchelor, initiated a large scientific activity, directed towards accurate prediction of the mean size of a passive cloud released into idealized flows with known parameters.
The few exceptions, in which other aspects of the dispersion in flows with given parameters have been addressed, has been summarized by Csanady (1973). Along his wording, the academic respectability of the tradition, and even these exceptions, may obscure the fact that it is insufficient for some practical purposes. The practical applications of gas cloud behaviour is a main reason for working with this particular application of meteorology at all, so we should constantly try to direct our attention towards the most important aspects.

The practical application for this study is prediction of the hazard area following the accidental release of an explosive or toxic gas cloud. The prediction is to be based upon predicted (estimated) transport and flow parameters. Therefore, even if this is a commonly addressed problem, it is really non-standard compared to traditional diffusion theory. The objective is to obtain as small and accurately predicted hazard area as is "optimal", at a given risk. A specific purpose of the present study is to make different meteorological aspects of hazard area prediction sufficiently explicit so as to allow estimation of what aspects are the most important ones in obtaining a small predicted hazard area.

To be specific, it is assumed that the instantaneously generated cloud is small and the hazard is associated with instantaneous gas concentration χ above a certain limit χ_h. When dealing with instantaneous concentrations, there will be only little differences between the relative spread of this cloud and the relative lateral spread of a continuous plume. The scale is imagined to be associated with a maximum hazard time and along-wind distance ordering $T_h = O(10 \text{ min})$ and $\theta_1 = O(5 \text{ km})$, respectively.

Ideas about the relative importance of different meteorological aspects of hazard area prediction are obtained from the following observations (e.g. Lumely and Panofsky, 1965; Panchev, 1971; Pasquill, 1974): i) the spectra of atmospheric variables have most energy at the larger scales, ii) the atmospheric eddies that contribute most to the dispersion of a cloud are of the same dimensions as the cloud; iii) the atmospheric eddies that contribute most to the cloud's centre of gravity motion are larger than the cloud; iv) cloud behaviour varies considerably with the flow parameters. The first three statements indicate that the size of the predicted hazard area depends more upon the prediction error for the centre of gravity location than on cloud dispersion. The last statement suggests that the size of the predicted hazard area depends much on the estimation errors for actual flow parameters. Analogous arguments apply to similar problems related to air pollution, and the ideas may appear obvious to some. Nevertheless, since the literature on approaching such problems is strongly biased towards diffusion models, they should be discussed in a more explicit form.

Although the problem setting may be suited for a Bayesian approach, conventional statistics is used for the exploratory purpose of this study. A modified intepretation of the transport variable in Gifford's (1959) fluctuating plume model is sufficient for applying Gifford's and Csanady's results to the description of the concentration field resulting from a cloud, given the flow parameters, and now a <u>prediction</u> of the actual centre of gravity transport (Section, 2). This framework is used to synthesize (parameterize) hazard area prediction based on the above information (Sections, 3a, 3b). The uncertainty associated with predicting the flow parameters is then accounted for, choosing unfavourable values (Section, 3c). This model is used to outline the importance of main meteorological aspects in obtaining a small predicted hazard area (Section, 4). The limited space available does not allow a complete treatment of this large subject.

2 Concentration distribution

The hazard probability depends on the stochastic concentration field in space and time $\chi(\underline{x},t)$. A complete statistical description of this non-homogeneous and non-stationary field is beyond reach. An aspect on which there is some information is the probability function of concentration at fixed spatial and time coordinates $F(\chi;\ \underline{x},t)$. This distribution is therefore chosen as the basis for this discussion. It is implicitely considered to be a function of atmospheric flow parameters.

It is convenient to discuss the spreading of a cloud in terms of the centre of gravity motion and the relative dispersion (Gifford, 1959). With source strength Q and the Lagrangian centre of gravity velocity $\underline{u}$, the centre of gravity vector $\underline{c}(t)$ is:

$$\underline{c}(t) = Q^{-1} \int \underline{x}\ \chi\ (\underline{x},t)d\underline{x}$$

$$= \int_{0}^{t} \underline{u}(\underline{c}(\tau))d\tau. \qquad (1)$$

The probability density for the stochastic $\underline{c}$ vector is $\beta(\underline{c},t)$. The conditional probability density for concentration at fixed spatial and time coordinates, given the centre of gravity vector,

$\beta(\chi;\ \underline{r},t) = \beta(\chi/\underline{c};\ \underline{x},t)$; $\underline{r} = \underline{x} - \underline{c}$, with conditional prabability $F(\chi;\ \underline{r},t)$. The joint density of the two stochastic variables, concentration and centre of gravity vector, is then $\beta(\chi,\underline{c};\ \underline{x},t) = \beta(x;\underline{r},t)\ \beta(\underline{c};t)$, so that the marginal probability of interest becomes (Csanady, 1973):

$$F(\chi;\underline{x},t) = \int F(\chi;\underline{r},t)\beta(\underline{c};t)d\underline{c}\ . \tag{2}$$

a. <u>Conditional concentration distribution</u>. Experimental evidence (Csanady, 1973) indicates that the conditional concentration distribution $F(\chi;\ \underline{r},t)$ may be represented reasonably well by 3 parameters: the probability of zero concentration, $F(0;\underline{r},t)$, and the parameters $\chi_o(\underline{r},t)$ and $\sigma_*(\underline{r},t)$ of a lognormal distribution for nonzero concentrations.

$$F(\chi;\underline{r},t) = \begin{cases} F(0) & ,\ \text{for}\ \chi = 0 \\ \frac{1}{2}\left[1+\text{efr}\left(\frac{\ln\chi/\chi_o}{\sqrt{2}\ \sigma_*}\right)\right] & ,\ \text{if}\ \ \chi > 0 \end{cases} \tag{3}$$

As mentioned, most studies of turbulent diffusion are concerned with properties of the first moment $\bar{\chi}(\underline{r},t)$ of $F(\chi;\ \underline{r},t)$. For a passive scalar cloud this moment is commonly found to have spatially Gaussian profiles for $|\underline{r}| \lesssim O(2\sigma_1)$. With proper orientation of coordinate axes, the $\bar{\chi}$-field may then be discussed in terms of standard deviations, $\sigma_i(t)$; i = 1, 2, 3. Assuming isotropy, Smith and Hay's (1961) diffusion model illustrates the dependence between dispersion and flow parameters

$$\frac{d\sigma_1}{dt} \simeq \frac{3}{U}\int_0^\infty \phi(k)\kappa(k)dk; \tag{4}$$

$$\kappa(k) = (\sigma_1 k)^{-1}[1-e^{-(\sigma_1 k)^2}] \tag{5}$$

The flow parameters are the mean wind, U, and the small scale Eulerian three-dimensional wave number turbulence spectrum $\phi(k)$, with integral scale L=O(100 m). The transfer function, $\kappa(k)$, shows that the most efficient atmospheric eddies to disperse the cloud have the same dimensions as the cloud itself. Eqs. (4) and (5) give approximately (Pasquill, 1974):

$$\frac{d\sigma_1}{dt} \simeq 0.2\ \sigma_u, \quad \text{for } \frac{\sigma_1}{L} \leq O(1), \tag{6}$$

so that a small cloud grows approximately linearly with time. Eqs. (4), (5) and (6) indicate that only a small part of the turbulence spectrum is active in cloud dispersion at a given time. With surface roughness, z_o (in metres), the following closure equation is commonly estimated as reasonably accurate:

$$\sigma_u \simeq \left(\ln \frac{10}{z_o}\right)^{-1} U \quad = O(0.1\ U) \tag{7}$$

Estimates for $F(0;\underline{r},t)$ and $\sigma_*(\underline{r},t)$ are associated with large uncertainty (Csanady, 1973; Eidsvik, 1980 b). Here it is assumed that $F(0) < O(10^{-1})$ and $\sigma_*(r) \simeq 0.5$ in the interior of the cloud.

The joint properties of χ are generally unknown. However, it appears that the probability of simultaneous high (or low) concentrations at two locations closer together than the expected cloud size tends to be high (Eidsvik 1980 b).

b. <u>Centre of gravity prediction error distribution</u>. In Gifford's and Csanady's works the (horizontal) $\underline{c}$ of (2) is measured relative to its expectation, unknown in case of an accidental gas release. The information that can be obtained is a prediction of the centre of gravity transport:

$$\hat{\underline{c}}(t) = \int_0^t \hat{\underline{u}}(\hat{\underline{c}}(\tau))d\tau \simeq \hat{\underline{u}}t. \tag{8}$$

Here $\hat{\underline{u}}$ is the predicted atmospheric wind along the predicted trajectory. Since it may be difficult to estimate $\underline{u}$ significantly more accurately than to be constant over horizontal coordinates and times of the order $(Ut,t) < O(5\text{ km}, 10\text{ min})$, (Eidsvik,1978,1981), the approximation in (8) is most probably allowed. The prediction error is:

$$\begin{aligned} {}'\underline{c}(t) &= \underline{c}(t) - \hat{\underline{c}}(t) \\ &= \int_0^t [\underline{u}(\underline{c}(\tau)) - \hat{\underline{u}}(\hat{\underline{c}}(\tau))]d\tau \\ &\simeq \int_0^t [\underline{u}(\hat{\underline{c}}(\tau)) - \hat{u}(\hat{\underline{c}}(\tau))]d\tau. \end{aligned} \tag{9}$$

Since the extrapolation distances in space and time associated with this prediction of $\underline{c}$ are normally much larger than the difference between $\underline{c}$ and $\hat{\underline{c}}$, the transcendental and Lagrangian character of (9) may, for the purpose of this study, be avoided by replacing $\underline{c}$ with $\hat{\underline{c}}$ on the right hand side. It is convenient to consider $\underline{x}$ and $\underline{c}$ to be vectors in a coordinate system moving with $\hat{\underline{c}}$ and orient the system so that the 1-axis is along the predicted, but not necessarily constant wind $\hat{\underline{u}}(t)$.

The distribution of the prediction error for the centre of gravity location is then $\beta('\underline{c};t)$. With this interpretation, Gifford's and Csanady's results are applicable to describe dispersion statistics given the flow parameters and a prediction of the actual transport. A main result is that $F(\chi;\underline{x},t)$ depends much upon $\beta('\underline{c},t)$. A simple but important new point is that $\beta('\underline{c};t)$, and therefore $F(\chi;\underline{x},t)$, can now be controlled (i.e. regulated) by means of the prediction method for $\underline{c}$. Since the available time for prediction is smaller than the diffusion time $t = O(10$ min.), the prediction method must be based upon simple use of local information about the atmospheric flow. The best conceivable prediction is most likely comparable to the prediction obtained by tracking a dummy cloud released at approximately the same (time and space) location as the actual. The prediction error associated with this may be thought of as the result of two-particle diffusion. For the prediction to be of any use, it must be based upon tracking data up to a much less time than the maximum hazard time. Extrapolation over a sufficiently long lead time must add to give a minimum prediction error that is significantly larger than σ_1 of (4). Realistic prediction methods must give larger errors.

In order to estimate more realistic lower limits to the predictability of $\underline{c}$, the cloud trajectory is assigned to the coordinate of its predicted centre of gravity over the diffusion time, $(\underline{x}_o,t_o)$. Measurements occur at the coordinates $(\underline{x}_i;\ t_i<t_o)$; $i = 1, 2, ..$ Using $||\cdot||$ as notation for a norm or a typical value, the the minimum resolution of this idealisation may be expressed as $||\Delta x,\ \Delta t|| = O||Ut,\ t|| \geq O(L) = O(100\text{ m})$, i.e. it is not

appropriate for a discussion of small scale effects. However, the energetic atmospheric fluctuations have larger scales so that (9) may be approximated as:

$$'\underline{c} \simeq t[\underline{u}(\underline{x}_o,t_o) - \hat{\underline{u}}(\underline{x}_o,t_o)]. \qquad (10)$$

The minimum prediction error may then be discussed in terms of optimal interpolation and extrapolation of the atmospheric (larger scale) field $\underline{u}(\underline{x},t)$. This is, in principle, a question of stochastic models for field variables, a subject in its infancy for field dimensions higher than one (Granger, 1975). However, guidance from time-serie analysis and Gandin's (1965) theory for optimal interpolation and extrapolation when the measurement setup is given, may be used to estimate how the prediction error may be most efficiently minimized. Without going into details on this, a main result from these theories, as applied to atmospheric flucutations, is generally that nothing is more efficient in producing accurate predictions than a measurement close to the coordinate for which the prediction shall be used (Eidsvik, 1978, 1981). When the prediction method needs to be specified, we will therefore assume that only the nearest measurement is used. With additive, combined effects from small scale turbulence and measurement error $\underline{\varepsilon}(\underline{x}_1,t_1)$, the prediction error for $\underline{c}$ then becomes approximately:

$$'\underline{c} \simeq t[\underline{u}(\underline{x}_o,t_o) - \underline{u}(\underline{x}_1,t_1) - \underline{\varepsilon}(\underline{x}_1,t_1)], \qquad (11)$$

so that the covariance matrice becomes

$$E'\underline{c}'\underline{c}^T \simeq t^2\{\underline{D}(\underline{x}_o - \underline{x}_1, t_o - t_1) + E\,\underline{\varepsilon}\,\underline{\varepsilon}^T\}. \tag{12}$$

Assuming $'\underline{c}$ to be nearly Gaussian with zero mean, (12) exemplifies how $\beta('\underline{c},t)$ may be controlled by the prediction method, by varying $\underline{x}_1, t_1$ and $E\,\underline{\varepsilon}\,\underline{\varepsilon}^T$. The diagonal terms of the structure function matrice, $\underline{D}$, is estimated to increase approximately linearly with its arguments for $L << |\underline{x}_o - \underline{x}_1| << 100$ km and $L/U << t_o - t_1 << 12$ hr (Panchev, 1971). For realistic minimal $|\underline{x}_o - \underline{x}_1| = O(Ut)$, $t_o - t_1 = O(t)$ and $||\underline{\varepsilon}|| \simeq \sigma_u$, it follows that $||E'\underline{c}'\underline{c}^T|| \geq t^2\,\sigma_u^2$, so that using (6) gives:

$$\frac{||E'\underline{c}'\underline{c}^T||}{\sigma_1} \geq O\left(\frac{\sigma_u}{0.2\sigma_u}\right) \simeq O(5). \tag{13}$$

Apart from being an order of magnitude estimate, this equation also indicates that $||E'\underline{c}'\underline{c}^T||$ is associated with larger atmospheric scales than σ_1. The filtering of large scale atmospheric fluctuations by the prediction method for $\underline{c}$ is further illustrated, noting that the structure function of a scalar, along one spatial coordinate y is:

$$D(y) \propto \int_0^\infty \phi(k_y)\,\sin^2\frac{k_y \cdot y}{2}\,d\,k_y, \tag{14}$$

with $\phi(k_y)$ the one-dimensional spectrum along the y-direction (Panchev, 1971). According to (14) the contributions from atmospheric eddies of larger dimensions than y are damped. However, since $\phi(k_y)$ has most energy at low wavenumbers, the atmospheric eddies that contribute most to the prediction error are of approximately the same dimensions as the distance (in time and space) between the nearest measurement and the centre of gravity for the cloud trajectory. This distance will normally be much larger than σ_1, so that the eddies contributing for $E'\underline{c}'\underline{c}'^T$ are of much larger scales than those contributing to σ_1 (4,5).

The picture of cloud dispersion given the flow parameters and predicted transport, summarized in this chapter, is illustrated in Figure 1.

3 Actual and predicted hazard area

This picture will now be used to syntesize (parametrize) hazard area prediction, given the flow parameters and a transport prediction. For simplicity, the main objective is specified to a prediction of the area which may be affected by hazardous concentrations at some time following the release. The actual realization of hazard occurs in a stochastic area around $'\underline{c}(t)$ where $\chi > \chi_h$, illustrated by the shaded area in Figure 1. Hazard must be predicted in the area where the distribution $F(\chi_h;\underline{x},t)$ (or $F(\chi_h;\underline{x},t)$ at some time), given a transport prediction, exceeds an unacceptable value. Since the predicted hazard area must be geometrically simple, it is sufficient to discuss simple aspects of the actual and predicted hazard area only.

a. Transverse dimension. Suppose that there exists an along-wind range, $x \simeq Ut$, such that $\chi_o(r=0) \gg \chi_h$ for all $\sigma_1(t=0) \ll x \ll \theta_1$. Since the probability of simultaneously high (or low) concentration at two locations closer together than the expected size of the cloud is estimated to be high (Eidsvik, 1980b), most of the actual hazard is confined to a compact region around the location of the actual gravity centre in this interval of x (as illustrated in Figure 1). The most important aspect of the hazardous concentration field then appears to be represented with an ellipse of "optimal" shape and orientation, or more simply a circle of radius s. With the Heavyside function H, s may be expressed as (compare Csanady, 1969):

$$\Pi s^2(t) = \int H(\chi(r_1,r_2,0,t) - \chi_h)dr_1dr_2 \tag{15}$$

$$\simeq \int H(\chi)\ dr_1dr_2 \qquad ; \quad \text{for } \chi_o(r=0) >> \chi_h$$

The last approximation is based upon the assumption that in a neighbourhood where $\chi_o(r=0) >> \chi_h$, the probability of $\chi > \chi_h$ is unacceptably high, once $\chi > 0$. Since $H(\chi-\chi_h) = 0$ with probability $F(\chi_h;\underline{r},t)$ and $H(\chi-\chi_h) = 1$ with probability $1-F(\chi_h;\underline{r},t)$, $E\{H(\chi-\chi_h)\} = 1 - F(\chi_h;\underline{r},t)$ so that:

$$E\Pi s^2(t) = \int[1 - F(\chi_h;\underline{r},t)]\ dr_1dr_2 \tag{16}$$

$$\simeq \int[1 - F(0;\underline{r},t)]dr_1dr_2 \ ; \ \text{for } \chi_o(r=0)>>\chi_h.$$

The large uncertainty associated with $F(0;\underline{r},t)$ and therefore, the stochastic structure of s cannot be avoided and implies that simple estimation should be used. The dominance of the large scale eddies in the atmosphere, implying a large $||c||$ compared to $||s||$, is another argument for this (13). Instead of trying to estimate $\mu_s(x_1) = (Es^2)^{\frac{1}{2}}$ using (16) (compare Csanady, 1969), estimates for the purpose of this study are obtained by means of the distance to a given mean concentration,

$\bar{\chi} \lesssim \chi_h$, in a conventional, three-dimensional isotropic Gaussian diffusion equation. This equation is solved with respect to the distance from the centre, r, to a concentration $\bar{\chi}$, and differentiated with respect to σ_1 (a monotonic function of x) to give the maximum hazard radius for the mean cloud, r_{max}. The following relations hold at the r-maximum:

$$\sigma_1(x) = (2\Pi e)^{-\frac{1}{2}} (Q/\bar{\chi})^{-1/3} \qquad ; \; r_{max} = \sqrt{3}\,\sigma_1(x). \quad (17)$$

The expected cloud becomes nonhazardous, r=0, at a σ_1-value $\sqrt{e} \approx 1.65$ times larger than this. For an appropriate choice of $\bar{\chi} \lesssim \chi_h$, the maximum μ_s is most probably comparable to r_{max}, comparable to $\sigma_1(x)$ for x somewhere in the interval $\sigma_1(t=0) << x << \theta_1$. Representative values for the difference between the parameters $\mu_s(x), \sigma_1(x)$ and $\{E'c_2^2(x)\}^{\frac{1}{2}}$ are shown in Figure 2. The higher moments of s require estimates of joint properties for the χ-field, which are even more uncertain. For simplicity it is here assumed that s is nearly normal, $n(\mu_s, \sigma_s)$, with mean μ_s and standard deviation, reasonably of the order $\sigma_s = O(\mu_s)$ in the interval $\sigma_1(t=0) << x << \theta_1$.

The predicted, instantaneous hazard area could be defined as the circle with radius $\theta_2(t)$, around the predicted location of the centre of gravity, such that the probability of hazard outside this circle is smaller than $\Pr\{s(t)+|\underline{c}(t)|>\theta_2\} = P_h$. When, as here, the interest is mainly on the transverse dimension of the predicted hazard area, $|'\underline{c}(t)|$ is replaced by the transverse component $'c_2(t)$. With the previous assumptions $(s + 'c_2)$ is $n(\mu_s;\sigma)$, $\sigma^2 = \sigma_s^2 + E'c_2^2$, so that θ_2 is obtained as:

$$\int_{0}^{\theta_2} n(\mu_s,\sigma)\,d\tau = \tfrac{1}{2}(1-P_h)$$

$$\int_{0}^{\frac{\theta_2-\mu_s}{\sigma}} n(0,1)\,d\tau = \tfrac{1}{2}(1 - P_h),$$

$$\operatorname{erf} \frac{\theta_2 - \mu_s}{\sqrt{2}\sigma} = (1 - P_h)$$

$$\theta_2(x) = \mu_s(x) + \sqrt{2}\sigma(x)\operatorname{erf}^{-1}(1 - P_h)$$

$$= \mu_s(x) + \sqrt{2}\alpha_2\sigma(x)$$

$$\theta_2(x) \simeq \sqrt{2}\alpha_2\{E\ c_2^2(x)\}^{\frac{1}{2}} \tag{19}$$

with $\alpha_2 = \operatorname{erf}^{-1}(1-P_h)$. The subscript is used to indicate two-sided probability. If risks of the order $P_h \simeq O(10^{-1})$ are accepted, $\alpha_2 \simeq 2$. Even at the particular x-value where μ_s reaches its maximum value (comparable to a $\sigma_1(x)$) the last approximation in (19) is valid (13, 17). This implies that the transverse dimension of the predicted hazard area is dominated by the prediction error, $\{E'c_2^2(t)\}^{\frac{1}{2}}$, exemplified by (12) at <u>all</u> distances $\sigma_1(t=0) << x$.

For fixed $(\underline{x}_1,t_1)$, t_o and therefore $D(\underline{x}_o-\underline{x}_1,\ t_o-t_1)$ increases slightly with t so that $\{E'c_2^2(t)\}^{\frac{1}{2}}$ will at least increase linearly with t (or x). This curvature of transverse hazard area limits is unusual compared to the picture obtained from diffusion models. The physical reason is different assumptions and filtering of the larger scale atmospheric fluctuations. In traditional diffusion models, too energetic larger scale flucuations (integral scale) are not allowed.

b. Maximum hazard distance. The maximum hazard distance should also be discussed via s(t) of (15), or rather by means of the last passage time to the state s(t) = 0. The distribution of the last passage time would, in principle, be given if a model of the nonstationary stochastic process s(t) or $\chi_{max}(t)$, existed. It has not been advanced, so that a simpler procedure have to be chosen. In the spirit of Lagrangian diffusion theory, the time and not along-wind spatial coordinate is assumed to be the most relevant variable for turbulent diffusion. The predicted maximum hazard distance, θ_1, is therefore discussed via the time, T_h, it takes before the probability for $\chi > \chi_h$ in the most hazardous, central portion of the cloud becomes small enough, $F(\chi = \chi_h; \underline{r} = 0, T_h) = P_h$. In the central portion of the cloud the intermittency factor is small, so that the concentration distribution is approximately log-normal. Analogous to the derivation of (19), this gives (compare Csanady, 1969, 1973):

$$\frac{\chi_h}{\chi_o} = \exp\ (\sqrt{2}\alpha_1\sigma_*), \tag{20}$$

with $\alpha_1 = \mathrm{erf}^{-1}\ (1-2P_h)$. The subscript is used to indicate one-sided probability. Eq. (20) may be written in terms of the mean value $\bar{\chi}$, instead of χ_o and inverted (compare Csanady, 1973):

$$\begin{aligned} T_h &= \bar{\chi}^{-1}\ \{\chi_h \exp[-\sqrt{2}\alpha_1\sigma_* + \tfrac{1}{2}\sigma_*^2]\} \\ &\simeq \bar{\chi}^{-1}\ \{\chi_h \exp[-\sqrt{2}\alpha_1\sigma_*]\}. \end{aligned} \tag{21}$$

The maximum hazard distance is, to first order, (compare 13, 19), determined by how far the cloud has been transported during this time, i.e., predicted transport $\hat{\underline{c}}(T_h)$ plus prediction error $\underline{'c}(T_h)$. Specifically, θ_1 is determined as the distance exceeded with probability P_h:

$$\theta_1 \approx \int_0^{T_h} \hat{u}(\tau)d\tau + \sqrt{2}\alpha_1\{E'c_1^2(T_h)\}^{\frac{1}{2}}$$

$$\approx \hat{u}_1 T_h + \sqrt{2}\alpha_1\{E\ c_1^2(T_h)\}^{\frac{1}{2}}. \tag{22}$$

c. Predicted hazard area. A reasonably rational and simple way to estimate the predicted hazard area in an atmosphere with known flow structure and predicted transport has now been developed. The predicted hazard area is characterized by θ_1 of (22), and θ_2 of (19). The quantile $\underline{\theta} = \{\theta_1, \theta_2\}$ of the approximate order $1 - P_h$, depends upon the atmospheric diffusion parameter vector $\underline{\mu} = \{F(0), \sigma_i, \bar{\chi}, \sigma_*, E'c_i^2;\ i = 1,2\}$, through the equations developed. The diffusion parameters depend in turn on the atmospheric flow parameter vector of (4) and (12), $\underline{\nu} = \{U, \underline{\phi}(\underline{k}), \underline{D}(\underline{x})\}$, so that the relations may formally be written:

$$\underline{\theta} = \underline{\theta}(\underline{\mu}(\underline{\nu})). \tag{23}$$

In an actual situation of gas release, the parameters must be estimated (predicted). The available information will be a prediction of atmospheric flow parameters, $\hat{\nu}_k$. For hazard estimation, an unfavourable parameter must be chosen, say $\tilde{\nu}_k$ (conditional worst case):

$$\tilde{\nu}_k = \hat{\nu}_k \pm \Delta\nu_k. \tag{24}$$

To be specific, $\hat{\nu}_k$ is imagined to be nearly normally distributed, so that the unfavourable $\Delta\nu_k$ is selected at the risk level $P_h^* = O(P_h)$ as $\Delta\nu_k \simeq \sqrt{2}\alpha_1^*\{E[\hat{\nu}_k - E\hat{\nu}_k]^2\}^{\frac{1}{2}}$, with $\alpha_1^* = \text{erf}^{-1}\ (1-2P_h^*) \simeq \alpha_1$. The minus sign is chosen when a small ν_k is most hazardous. Except for σ_*, the components of dispersion models, $\hat{\underline{\mu}}(\underline{\nu})$, have received much attention. Model errors have been discussed by Pasquil (1974) and Hanna et al. (1978). In "ideal conditions" an optimistic 10% relative accuracy for the cloud standard deviation seems to be appropriate. This gives ca 30% relative accuracy for the maximum mean concentration of an instantaneously generated cloud so that the diffusion model uncertainty in the time to a given mean concentration becomes approximately 10%. That is, the predicted maximum hazard time "safety factor" due to dispersion model inaccuracy of the "best mean" models is approximately 1.1 or so. With given $\Delta\nu_k$, a small diffusion model error may not necessarily result in a small prediction error for μ_i. This may be so if the "real" μ_i varies much over intervals of ν_j smaller than $\Delta\nu_j$. Several authors have indicated that the turbulent structure may actually have such a property in the neighbourhood of the commonly occuring "near neutral conditions" (Busch, 1973). It is, for instance, estimated that the "real" u_2-spectrum varies considerably from slightly positive to slightly negative Richardson numbers. When the prediction inaccuracy for Richardson number, ΔR_i, is comparable to or larger than this interval, the prediction accuracy for the u_2-spectrum (and therefore turbulent diffusion) could be better with a spectrum model that is smooth over ΔR_i-intervals than with a "realistic". For the purpose of this study, the dispersion model is assumed to be very accurate:

$$\underline{\tilde{\theta}} = \underline{\hat{\theta}}(\underline{\hat{\mu}}(\underline{\tilde{\nu}})) = \underline{\hat{\theta}}(\underline{\tilde{\mu}}), \tag{25}$$

It is understood that $\tilde{\mu}_i = \hat{\mu}_i(\underline{\tilde{\nu}})$ when models exists, and $\tilde{\sigma}_* = \hat{\sigma}_* + \Delta\sigma_*$ for $\mu_i = \sigma_*$. Since the ~ operator is not necessarily commutative with respect to other operators appearing in (25), the relation is not unique. However, a reasonable interpretation is sufficient for the present purpose. Application of (24) and (25) to (19), (21) and (22) give:

$$\tilde{\theta}_2(x) \simeq \sqrt{2}\alpha_2 \widetilde{[E'c_2^2(x)]^{\frac{1}{2}}},$$

$$\simeq \sqrt{2}\alpha_2[\widetilde{\{E'c_2^2(x)\}}^{\frac{1}{2}} + \Delta\{E'c_2^2(x)\}^{\frac{1}{2}}] \tag{26}$$

$$\tilde{T}_h \simeq \tilde{\tilde{\chi}}^{-1}\{\chi_h \exp[-\sqrt{2}\alpha_1\tilde{\sigma}_*]\}, \tag{27}$$

$$\tilde{\theta}_1 \simeq \hat{u}_1\tilde{T}_h + \sqrt{2}\sigma_1 \widetilde{\{E'c_1^2(\tilde{T}_h)\}^{\frac{1}{2}}} \tag{28}$$

For clouds that are initially large, or rapidly becomes so, such as "heavy gas clouds (Eidsvik, 1980a), (26) and (28) should have an additive correction term of the order of σ_1. Apart from this, important aspects of hazard area prediction seems to be synthesized by (26, 27 and 28) also for these clouds. $\tilde{\theta}_1$ and $\tilde{\theta}_2$, depend, to first order, upon the prediction error for wind given the flow parameters and prediction error for these parameters. In addition $\tilde{\theta}_1$ depends implicitely upon the turbulent diffusion through the predicted maximum hazard time $\tilde{T}_h$.

4 Characteristic values

For a given approximate risk (P_h or $P_h \cdot P_h^*$) the control variables for making the size of the predicted hazard area small are: $E'c_i^2(t)$, $\bar{\chi}(r=0;\ \tilde{\underline{\nu}})$ and $\tilde{\sigma}_*$. The discussion of their effectiveness is a broad subject, that can only be outlined here.

a. Transverse dimension. With the use of an error-free measurement, responsive to small scale turbulence, located at the gas release location (26) reads, to first order:

$$\tilde{\theta}_2\ (x) \simeq \sqrt{2}\alpha_2[D_{22}(t_o - t_1) + \sigma_u^2]^{\frac{1}{2}}. \tag{29}$$

The half angle spanned by the predicted hazard area is then

$$\frac{\tilde{\theta}_2(x)}{x} \simeq \sqrt{2}\alpha_2 \frac{[D_{22}(t_o - t_1) + \sigma_u^2]^{\frac{1}{2}}}{U}. \tag{30}$$

Although the estimation of this variable is a traditional problem, (30) appears to be the first example of a reasonably explicite way. The benefit of a short lead time in the prediction is determined by the atmospheric structure. Since D_{22} is estimated to be approximately proportional to the time $(t_o - t_1)$ for $O(1\ \text{hr}) < t_o - t_1 < O(12\ \text{hr})$, (Panchev, 1971), the last term of (30) is typically as illustrated in Figure 3. The benefit of a short lead time is obvious. At the risk level $P_h \simeq 0.1$, $\alpha_2 \simeq 2$, so that the minimum angle must be ca 15^o, which appears to be representative for most ad hoc estimates. As indicated by (7) and (30), it varies considerably with the flow.

b. <u>Maximum hazard distance</u>. The expected size of an initially small passive scalar cloud increases approximately linearly with the time, (6), so that the expected maximum concentration decreases approximately as:

$$\bar{\chi}(t) \propto \frac{Q}{\sigma_u^3} t^{-3}. \tag{31}$$

Introduced into the inverted version of (27):

$$\frac{Q}{\tilde{\sigma}_u^3} \tilde{T}_h^{-3} \propto \chi_h \exp[-\sqrt{2}\alpha_1 \sigma_*], \tag{32}$$

this gives the predicted hazard time

$$\tilde{T}_h \propto \left[\frac{\tilde{Q}}{\chi_h}\right]^{1/3} \left[\exp\left(\frac{\sqrt{2}\alpha_1}{3} \tilde{\sigma}_*\right)\right] \left[\frac{1}{\tilde{\sigma}_u}\right]$$

$$\frac{\tilde{T}_h}{T_h} \simeq \left[\frac{\tilde{Q}}{Q}\right]^{1/3} \left[\exp \frac{\sqrt{2}}{3} \alpha_1 \tilde{\sigma}_*\right] \left[\frac{\sigma_u}{\tilde{\sigma}_u}\right], \text{ for } \sigma_1(T_h) \leq O(L). \tag{33}$$

Logarithmic variation of (33) indicates that $\tilde{T}_h$ varies less rapidly with prediction error for the released mass, Q, compared to prediction errors for σ_* and the flow parameters, σ_u. Figure 4 illustrates the variation with the prediction errors for σ_* and σ_u.

The increase in T_h due to concentration fluctuations and their uncertainty is given by the exponential term of (33). For $\hat{\sigma}_* \simeq \Delta\sigma_* \simeq 0.5$ and $P_h \simeq O(10^{-1})$, $\alpha_1 \simeq 2$, this "safety factor" for T_h then becomes approximately 1.5.

The increase in T_h due to prediction errors for actual flow parameters is likely to be large. Based on general experience from turbulence experiments in ideal homogenous and stationary flows, $\Delta\sigma_u/\sigma_u = O(1)$ is judged as representative for conventional estimation methods and commonly occurring flows. It is felt that lower limits for the flow parameter prediction error can hardly be made smaller than $\Delta\sigma_u/\sigma_u = 0.1$. The typical prediction errors may therefore, as seen from the last factor of (33), increase the predicted hazard time from T_h to $\tilde{T}_h$ by more than 2, with a lower limit of the order of 1.1. The predicted maximum hazard time may thus be much larger than the value obtained from conventional use of a most accurate diffusion model.

The predicted maximum hazard distance is exemplified as obtained from (22), (28) and (29):

$$\frac{\tilde{\theta}_1}{\theta_1} \simeq \{1 + \sqrt{2}\alpha_1[\frac{\overline{(D_{11}(t_o - t_1) + \sigma_u^2)^{\frac{1}{2}}}}{\hat{u}_1}]\} \frac{\tilde{T}_h}{T_h}$$

$$\simeq \{1 + \sqrt{2}\alpha_1[\frac{\overline{(D_{11}(t_o - t_1) + \sigma_u^2)^{\frac{1}{2}}}}{U}]\} \frac{\tilde{T}_h}{T_h} \qquad (34)$$

The first term is obtained as in (30) and illustrated in Figure 3; the second comes from (33) and is illustrated in Figure 4. Prediction errors for actual flow parameters may increase the predicted maximum hazard distance by a factor larger than 2, with a lower limit of the order of 1.3. These are large numbers in comparison to the safety factor of 1.1 or so, caused by the inaccuracy of the dispersion model, given the transport and flow parameters.

5 Concluding remarks

This exploratory study has shown that hazard area prediction following an accidental gas release should be based on the equations (26, 27 and 28).

As for the cloud characteristics, nontraditional aspects associated with the (unknown) stochastic structure of hazardous cloud size, s(t), appears to be the most relevant for the present purpose. The accurate prediction of cloud standard deviation, given the flow parameters, is not sufficent for obtaining small and accurate predicted hazard area. Flow prediction errors may result in so large uncertainty of the predicted hazard distance that the simplest (traditional) diffusion models may be accurate enough. With a given, representative prediction error for flow parameters, it could even be that an accurate and detailed dispersion model gives a larger predicted hazard area than a less accurate one.

Concentration fluctuations and uncertainty about this may affect the along-wind dimension of the predicted hazard area as a safety factor of ca 1.5.

The prediction errors for the actual transport velocity, given the flow parameters and prediction errors for the actual flow parameters, have been estimated to affect the size of the predicted hazard area considerably. Representative flow prediction errors increase the linear dimensions of the predicted hazard area by a factor larger than 2. Even the "best" prediction methods result in an increase of the order of 1.3 or so.

It seems that we should try to design flow prediction (estimation) methods so that the predicted hazard area can be made "optimally" small. The analysis did not indicate any natural and realistic optimal level for the prediction accuracy.

Acknowledgements. The encouragement of Prof. E. Spjøtvoll and the positive criticism of V. Vitols, Y. Gotaas and B. Ottar are appreciated. This work was supported by the Norwegian Petroleum Directorate, through Steering Committee for contingency planning on the Continental Shelf.

References.

Busch, N.E., Panofsky, H.A., Tennekes, H., 1973: Turbulence structure in the planetary boundary layer. *Bound.- Layer Meteor.* 4 211-264.

Csanady, G.T., 1969: Dosage probabilities and area coverage from instantaneous point sources on ground level. *Atmospheric Environment*. 3, 25-46.

Csanady, G.T., 1973: *Turbulent diffusion in the environment.* D. Reidel Publishing Company, Dordrecht, 248 pp.

Eidsvik, K.J., 1978: *On near optimal interpolation and extrapolation of atmospheric variables using a few measurement stations.* Technical note VM-295. Norwegian Defence Research Establishment, Kjeller, 30 pp.

Eidsvik, K.J., 1980a : A Model for heavy Gas dispersion in the Atmosphere. *Atmospheric Environment.* 14. 769-777.

Eidsvik, K.J., 1980b: Estimates of concentration fluctuations in an instantaneous plume. *"Atmospheric Environment".* 14. 1365-1369.

Eidsvik, K.J., 1981: On Optimal Prediction of Ekman Layer Fluctuations over short Lead Times. Submitted for publication.

Gifford, F.A., 1959: Statistical properties of a fluctuating plume dispersion model. *In: Atmospheric Diffusion and Air Pollution*, F.N. Frenkiel and P.A. Sheppard, Eds., Advance in Geophysics, vol. 6 Academic Press, New York, 117-136.

Lumley, J.L., Panofsky, H.A., 1964: *The structure of atmospheric turbulence.* John Wiley, New York, 239 pp.

Gandin, L., 1965: *Objective analysis of meteorological fields.* Hydrometeor. Publ. House, Leningrad, Translation Jerusalem, 242 pp.

Granger, C.W.J., 1975: Aspects of the Analysis and Interpretation of Temporal and Spatial Data. *The Statistican*, 24, 197-210.

Hanna, S.R., Crawford, T.V., Brendel, W.B., Deardorff, H.J.W., Horst, T.W., Fichtl, G.H., Randerson, D., Arya, S.P.S., Norman, J.M., 1978: Accuracy of Dispersion Models. *Bulletin American Meteorology Society*, 59, 1025-1026.

Panchev, S., 1971: *Random functions and turbulence.* Pergamon Press, New York, 444 pp.

Pasquill, F., 1974: *Atmospheric diffusion. The dispersion of windborne material from industrial and other sources.* John Wiley, New York, 429 pp.

Smith, F.B., Hay, J.S., 1961: The expansion of cluster of particles in the atmosphere. *Quart. J.R. Meteor. Soc.* 87, 82.

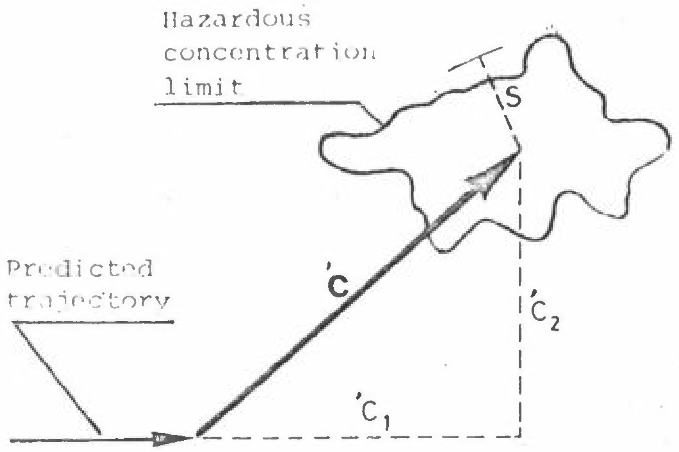

Figure 1: The prediction error for cloud location, $'\underline{c}$, is normally much larger than the hazardous cloud, of characteristic dimension, s.

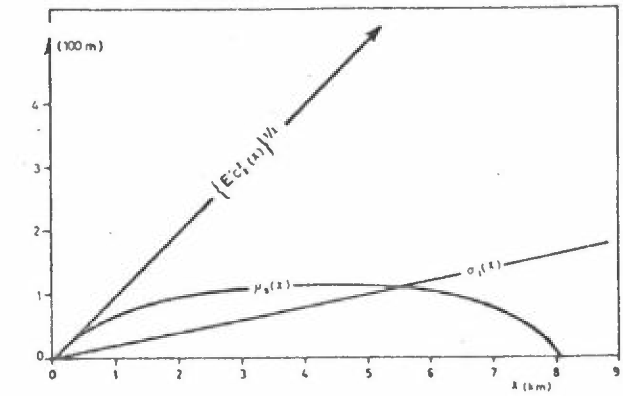

Figure 2: Schematic representation of the differences between cloud standard deviation, $\sigma_1(x)$, minimum prediction error for cloud location, $\{E'c_2^2(x)\}$, and mean size of the hazardous part of a cloud, $\mu_s(x)$.

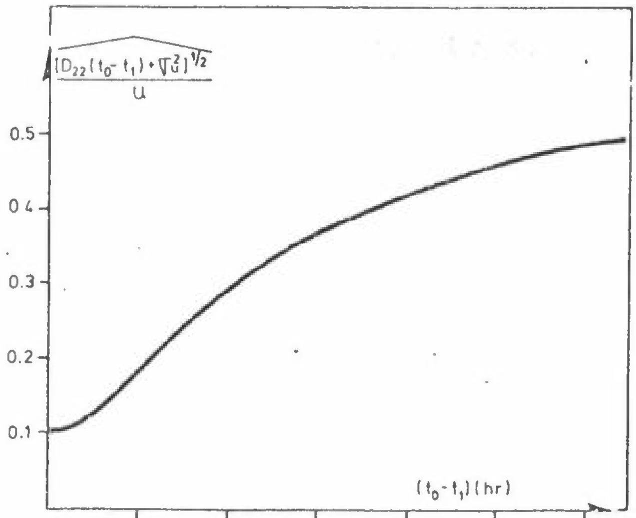

Figure 3: Schematic representation of the prediction error for cloud transport as a function of the lead time (see Eq. 30).

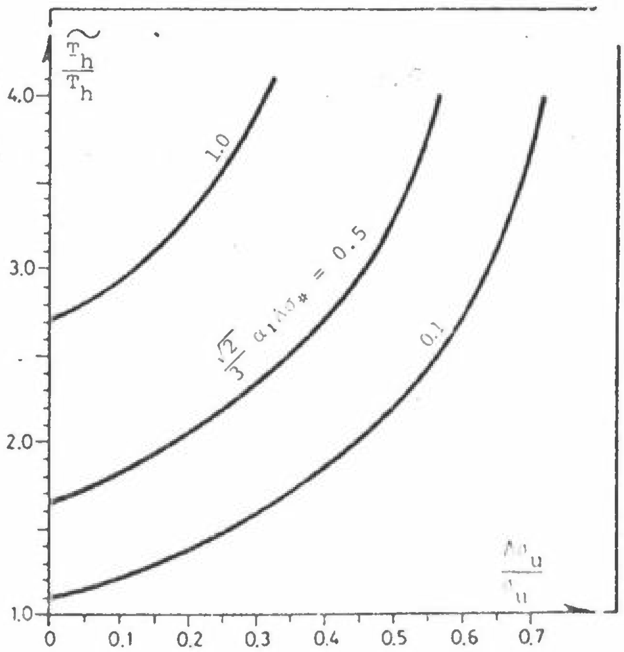

Figure 4: Safety factors for predicted maximum hazard time, $\tilde{T}_h/T_h$, due to prediction errors for concentration fluctuations, σ_*, and turbulence, σ_u (see Eq. 33).

NORSK INSTITUTT FOR LUFTFORSKNING

N I L U

(NORGES TEKNISK-NATURVITENSKAPELIGE FORSKNINGSRÅD)
POSTBOKS 130, 2001 LILLESTRØM
ELVEGT. 52.

TLF. (02) 71 41 70

RAPPORTTYPE OPPDRAGSRAPPORT	RAPPORTNR. OR 1/81	ISBN--82-7247- 214-7
DATO JANUARY 1981	ANSV.SIGN. B.Ottar B. Ottar	ANT.SIDER 25
TITTEL On the Prediction of hazard Area resulting from a Gas Release		PROSJEKTLEDER K.J. Eidsvik NILU PROSJEKT NR 22279
FORFATTER(E) Karl J. Eidsvik		TILGJENGELIGHET ** A OPPDRAGSGIVERS REF.
OPPDRAGSGIVER Oljedirektoratet		
3 STIKKORD (å maks.20 anslag) Gassutslipp	Varsling	Fareområde
REFERAT (maks. 300 anslag, 5-10 linjer)		
TITLE		

ABSTRACT (max. 300 characters, 5-10 lines)
A synthesis of hazard area prediction following the release of a hazardous gas cloud is developed. At a fixed risk level the predicted hazard area is estimated to depend much upon prediction errors for actual atmospheric transport and flow parameters.

**Kategorier: Åpen - kan bestilles fra NILU A
Må bestilles gjennom oppdragsgiver B
Kan ikke utleveres C